

## Is Sedna another Triton?\*

M. A. Barucci<sup>1</sup>, D. P. Cruikshank<sup>2</sup>, E. Dotto<sup>3</sup>, F. Merlin<sup>1</sup>, F. Poulet<sup>4</sup>, C. Dalle Ore<sup>5</sup>, S. Fornasier<sup>6</sup>, and C. de Bergh<sup>1</sup>

<sup>1</sup> LESIA, Observatoire de Paris, 92195 Meudon Principal Cedex, France  
e-mail: [antonella.barucci; frederic.merlin; catherine.debergh]@obspm.fr

<sup>2</sup> NASA Ames Research Center, MS 245-6, Moffett Field, CA 94035-1000, USA  
e-mail: Dale.P.Cruikshank@nasa.gov

<sup>3</sup> INAF-OAR Via Frascati 33, 00040 Monteporzio Catone (Roma), Italy  
e-mail: dotto@mporzio.astro.it

<sup>4</sup> IAS, Université Paris-Sud, 91405 Orsay Cedex, France  
e-mail: francois.poulet@ias.u-psud.fr

<sup>5</sup> SETI Institute, Mountain View, CA & NASA Ames Research Center, USA  
e-mail: cdalleore@mail.arc.nasa.gov

<sup>6</sup> Dipartimento di Astronomia, Vicolo dell'Osservatorio 2, 35122 Padova, Italy  
e-mail: fornasier@pd.astro.it

Received 30 May 2005 / Accepted 20 June 2005

**Abstract.** 90377 Sedna is, so far, the largest and most distant trans-neptunian object. It was observed at visible and near-infrared wavelengths using simultaneously two 8.2 m telescopes at the Very Large Telescope of the European Southern Observatory. The spectrum of Sedna suggests the presence on its surface of different ices (total abundance >50%). Its surface composition is different from that determined for other trans-neptunian objects, and apparently resembles that of Triton, particularly in terms of the possible presence of nitrogen and methane ices.

**Key words.** TNOs – visible – infrared – spectroscopy – photometry

### 1. Introduction

The Trans-Neptunian Objects (TNOs) are solid bodies orbiting the Sun beyond Neptune. The TNOs are extremely primitive remnants from the early accretional phase of the outer solar system and they may contain the most primitive and least altered material. The investigation of their surface composition is essential to understand the formation and evolution of this population, even though our knowledge of their physical properties is still limited by their faintness. Of all known solar system objects, Sedna has the largest perihelion distance, keeping it permanently in a very cold environment.

90377 Sedna (formerly 2003 VB<sub>12</sub>) has a semimajor axis of 501 AU, with perihelion and aphelion distances of 76 and 927 AU, respectively. With its perihelion distance more than twice the semimajor axis of Neptune, Sedna never enters the Kuiper Belt, and seems to belong to a dynamical separate class of objects different from all other known TNOs. After the discovery of 2000 CR<sub>105</sub> (semimajor axis 224 AU and perihelion distance 44 AU), a new TNO dynamical class called the “extended scattered disk”, which is beyond the range of interacting gravitational encounters with Neptune, had been hypothesized

(Gladman et al. 2002). Sedna is also beyond the scattering influence of Neptune, but its perihelion is much more distant.

### 2. Observations

We observed Sedna in the visible and in the near-infrared (imaging and spectroscopy) simultaneously using two 8.2 m telescopes (Antu and Kuyen) at the European Southern Observatory (Very Large Telescope, Cerro Paranal, Chile) on UT 2004 October 23 and 24. Sedna was at heliocentric distance 89 AU, and phase angle 0.25°. The visible imaging and spectral observations were carried out using FORS1 ([www.eso.org/instruments](http://www.eso.org/instruments)) simultaneously with some of the infrared observations. The near-infrared observations were obtained using ISAAC in its SW mode (for the spectroscopy). All the spectra, acquired using a 1-arcsec wide slit, were flattened, sky-subtracted and extracted using standard procedures (Barucci et al. 2002). To increase the S/N ratio, the observed near-infrared spectra ( $R = 500$ ) were smoothed by Gaussian filtering of  $\sigma = 15$  pixels. The night conditions were very good with the seeing averaging between 0.4–0.7 arcsec. The solar analog stars (HD and Landolt) were observed during the same night at the same airmass of each exposure; they are reported in Table 1 together with the relevant observational circumstances.

\* Based on observations collected at VLT Observatory Cerro Paranal of the European Southern Observatory, ESO in Chile, within the framework of programme 074.C-0121.

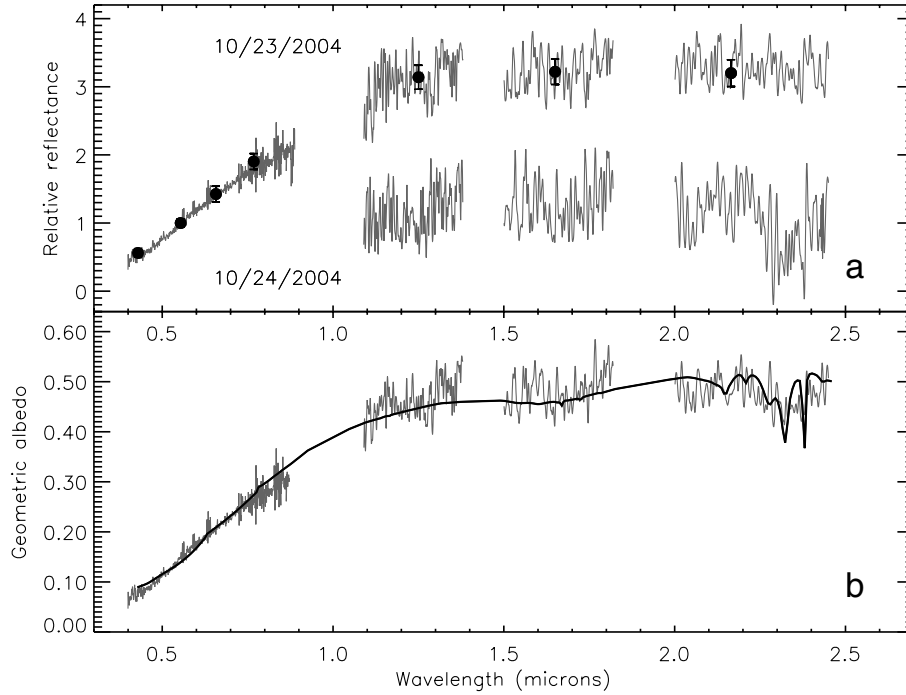


**Fig. 1.** **a)** Spectra of Sedna obtained on two different nights in the *V* (first night only), *J*, *H*, and *K* regions, with broadband photometric points at *B*, *V*, *R*, *I*, *J*, *H*, and *K* used to scale the individual segments of the spectra. The spectrum is normalized to 1 at  $0.55\ \mu\text{m}$ . The second night spectra have been shifted by 2 units for clarity. Assuming a rotational period of 10.27 h, the two *K*-band observations differ by about  $130^\circ$  in longitude. The strong absorption around  $2.3\ \mu\text{m}$  appears to be present only on one spectrum, while the band at  $2.15\ \mu\text{m}$  is present in both spectra. **b)** Co-added spectrum of Sedna with the best fit model (continuum line).

**Table 1.** Circumstances of the spectroscopic observations.

Date	UT (h:m)	Spec. reg.	Exp. (min)	Airmass	Solar analogs
10/23/04	5:30	<i>V</i>	30	1.18	HD 44594
10/23/04	6:00	<i>V</i>	30	1.16	HD 44594
10/23/04	6:40	<i>V</i>	30	1.19	HD 44594
10/23/04	4:22	<i>J</i>	42	1.29–1.23	L 115-271
10/23/04	5:20	<i>H</i>	60	1.22–1.16	L 115-271
10/23/04	6:35	<i>K</i>	60	1.16–1.22	L 115-271
10/23/04	7:40	<i>H</i>	60	1.23–1.41	L 115-271
10/23/04	8:40	<i>K</i>	48	1.41–1.7	HD 28099
10/24/04	4:40	<i>J</i>	36	1.25–1.2	L 93-101
10/24/04	5:18	<i>H</i>	42	1.18	L 93-101
10/24/04	6:23	<i>H</i>	48	1.17	L 93-101
10/24/04	7:30	<i>K</i>	54	1.22–1.4	L 93-101
10/24/04	8:30	<i>K</i>	48	1.4–1.7	HD 30246

The photometric calibration was performed by multiple observations of several visible and NIR standard stars.

### 3. Results

The mean visual magnitude (measured on October 24, 2004) is  $V = 21.32 \pm 0.05$  and the color indices are  $B - V = 1.23 \pm 0.09$ ,  $V - R = 0.76 \pm 0.09$ ,  $V - I = 1.37 \pm 0.07$ ,  $V - J = 2.32 \pm 0.06$ ,  $V - H = 2.61 \pm 0.06$ , and  $V - K = 2.66 \pm 0.07$ . The corresponding absolute magnitude is  $H = 1.8$ . Assuming

an albedo of about 0.15, Sedna's diameter is  $\sim 1500$  km. This implies that Sedna is the largest known object beyond Pluto, with a diameter estimated at two-thirds the size of Pluto. The measured color indices allow us to classify Sedna in the reddest group RR (Barucci et al. 2005)

The obtained spectra are shown in Fig. 1. The two traces in Fig. 1a show individual spectra from each night, and suggest variations in the surface composition. Assuming a rotational period of 10.27 h (Gaudi et al. 2005), the two spectra in Fig. 1a correspond to different surface regions on Sedna. The band at  $2.15\ \mu\text{m}$  is present in both spectra. The resolution of the spectra is 250 in the visible and 100 in the NIR. In order to increase the S/N ratio, we co-added the two individual spectra (Fig. 1b). Due to the long integration times used, this co-added spectrum corresponds to an average over a large part of Sedna's surface. In what follows, we analyse only this co-added spectrum.

The Sedna spectrum is very different from that of any other observed TNO, particularly in the *J*, *H* and *K* band regions. In fact all the other available TNO spectra in the near-infrared (Barucci et al. 2004; Jewitt & Luu 2004; Fornasier et al. 2004) are featureless or show absorption features of  $\text{H}_2\text{O}$  ice. The spectrum of Sedna shows a similarity to the spectrum of Triton (Fig. 2) in the  $2.0\text{--}2.5\ \mu\text{m}$  range (Cruikshank et al. 1993), in particular in terms of the presence of absorption bands of  $\text{N}_2$  and  $\text{CH}_4$ . These bands are also present in the Pluto spectrum, but in this case  $\text{CH}_4$  is much more abundant and the  $\text{N}_2$  band is barely visible (Owen et al. 1993).

The principal features of the spectrum of Sedna between  $2.0$  and  $2.45\ \mu\text{m}$  that appear to be reliable in view of

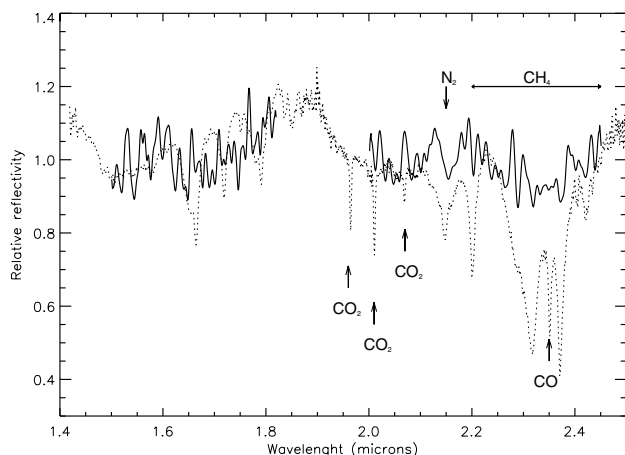


**Fig. 2.** *H* and *K* region spectra of Sedna (continuous line) and Triton (Cruikshank et al. 2000) (dotted line) shown at the same scale and normalized to 1 at  $1.65\ \mu\text{m}$ . The result of the cross-correlation of the two spectra is limited to the  $2.0\text{--}2.45\ \mu\text{m}$  region.

the statistical noise in the data include a prominent absorption band at  $2.15\ \mu\text{m}$  and a broad depression centered near  $2.3\ \mu\text{m}$  probably with some finer spectral structure. Triton has an absorption band at  $2.149\ \mu\text{m}$  identified as solid  $\text{N}_2$  in the  $\beta$  (hexagonal crystalline) phase. Dissolved in the solid  $\text{N}_2$  is a small amount of  $\text{CH}_4$  exhibiting a series of strong absorption bands and an overall depression of the continuum between  $2.2$  and  $2.5\ \mu\text{m}$  (Cruikshank et al. 1993). The  $\text{CH}_4$  on Triton also produces a series of three bands of moderate strength in the region  $1.5\text{--}1.8\ \mu\text{m}$ ; these bands are not apparent in the Sedna spectrum given their weakness. Not seen either in the Sedna spectrum are the broad water ice absorptions present in Triton's spectrum around  $1.5\text{--}1.6\ \mu\text{m}$  and  $1.9\text{--}2.1\ \mu\text{m}$ .

In order to test the similarities between the spectra of Sedna and Triton in a quantitative way, we have performed a cross-correlation study of these data, first isolating the  $2.0\text{--}2.45\ \mu\text{m}$  region where the absorption features are most prominent. Cross-correlation is a standard technique for the comparison of two signals (Becker et al. 2004). As one spectrum is incrementally displaced (in wavelength) with respect to the other, at each wavelength increment the sum of the product of the newly lined up amplitudes of the spectra is computed. The sum is large when the shift (delay) causes similar features in the two spectra to line up. For the cross-correlation we used the spectrum of Triton obtained with the 3.8-m United Kingdom Infrared Telescope at Mauna Kea on 13 and 15 May 1995, as used in the investigations by Quirico et al. (1999) and Cruikshank et al. (2000).

Triton's spectrum also has absorption bands of the ices of  $\text{CO}_2$  and  $\text{CO}$  (Fig. 2); these were ignored in the comparison with Sedna because the bands are very narrow and would not be expected to be distinguishable at the intrinsic noise level in the Sedna data. The results of the cross-correlation of the spectrum of Sedna with a  $\text{N}_2 + \text{CH}_4$  model (Fig. 3a; see caption of Fig. 3 for details), and the spectra of Sedna and Triton (Fig. 3b), show the peak power at (or very near) zero lag, giving a high level of confidence that the spectrum of Sedna has

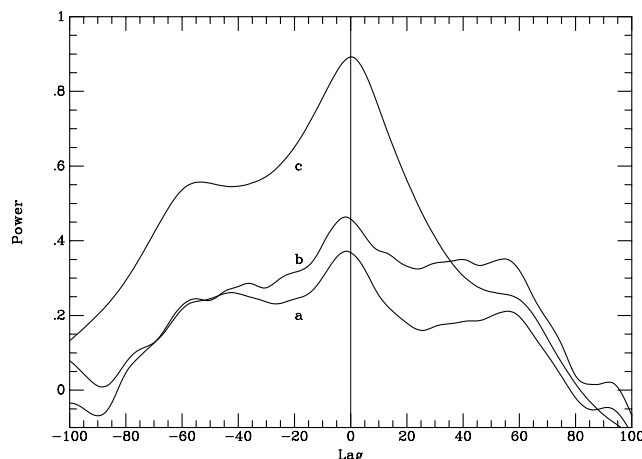


**Fig. 3.** Cross-correlation diagram for the wavelength region  $2.0\text{--}2.45\ \mu\text{m}$ . In each case the lag interval in wavelength was  $0.00038\ \mu\text{m}$ . **a)** Sedna spectrum versus a model calculated to provide an approximate match to the strengths of the  $\text{N}_2$  and  $\text{CH}_4$  bands. This model is not the same as shown in Fig. 1b, and was calculated with the code of Shkuratov et al. (1999) using 99.7% beta-phase  $\text{N}_2$  crystalline grains of  $700\ \mu\text{m}$  size, plus 0.3%  $\text{CH}_4$  dissolved in  $\text{N}_2$  in  $70\ \mu\text{m}$  grains. **b)** Sedna versus the Triton spectrum (described in the text). **c)** Triton versus the Sedna model described here. In all three cases, the maximum power peak at or very near zero lag shows that the spectral features in the spectrum of Sedna align favorably with the  $\text{N}_2$  and  $\text{CH}_4$  absorption bands in the spectrum of Triton. The broad pedestal in the power distribution between lag intervals of  $\pm 60$  arises from the noise in the Sedna spectrum.

the same main spectral bands ( $\text{N}_2$  and  $\text{CH}_4$ ) as that of Triton in the  $2.0\text{--}2.45\ \mu\text{m}$  region.

#### 4. Modelling

The modeling of the Sedna spectrum is done by using the radiative transfer theory developed by Shkuratov et al. (1999). In addition to common intimate mixtures, an intramixture can be formulated in which some individual large particles can contain a mixture of different materials visualized as small inclusions in the bulk, as might result from initially pure ice evolving in composition under the effects of space weathering and meteoritic bombardment. The non-icy contaminants can also be seen as an intrinsic material (Poulet et al. 2002). The data are fitted assuming a relatively low albedo typical for TNOs, and using a simplex minimization algorithm, in which abundance and grain size are free parameters for each component. The relevant absorption bands and the continuum shape of the spectrum are well reproduced (Fig. 1b) by an intimate mixture of five components: 24% Triton tholin, 7% amorphous carbon, 10%  $\text{N}_2$  ice, 26%  $\text{CH}_3\text{OH}$  ice and 33% of  $\text{CH}_4$  ice contaminated by small inclusions of Titan tholin (20%). The grain size of  $\text{N}_2$  is  $10\ \mu\text{m}$ , while for the other components the grains are about  $10\ \mu\text{m}$ . The corresponding albedo is 0.15 at  $0.55\ \mu\text{m}$ . The band at  $2.15\ \mu\text{m}$  attributed to the overtone band of solid nitrogen is well reproduced by a very long absorption path length (10 cm). If this long path length can be interpreted as grain size, a compact crystalline solid surface rather than granular surface is present on the surface (Quirico et al. 1999).

By contrast, the grain size of CH<sub>4</sub> and CH<sub>3</sub>OH ices is much smaller (less than 10 μm).

On Triton, most of the CH<sub>4</sub> is dissolved in the large crystals of N<sub>2</sub>, causing a shift of the main absorption bands to shorter wavelengths (compared to pure CH<sub>4</sub>) by some 0.007 to 0.014 μm (the matrix shift) (Cruikshank et al. 1993). The CH<sub>4</sub> abundance in N<sub>2</sub> is less than 1% on Triton; the bands are very prominent because of the long optical pathlength through the large N<sub>2</sub> crystals. In our Sedna data, the S/N is insufficient to allow us to distinguish the spectral shift between N<sub>2</sub>:CH<sub>4</sub> and pure CH<sub>4</sub>. However, the cross-correlation of the Sedna data with our Sedna models calculated with the matrix-shifted CH<sub>4</sub> bands show a smaller lag (near zero) than those calculated with models incorporating pure CH<sub>4</sub> and having no matrix shift.

The maximum predicted surface temperature of Sedna for ~200 years centered on its perihelion passage exceeds the 35.6 K temperature at which the low-temperature N<sub>2</sub> α phase transforms into the higher temperature β phase, which is the phase seen on Triton. Triton has a tenuous atmosphere that is in vapor-pressure equilibrium with the surface. The vapor pressure of β N<sub>2</sub> at 38 K is 14 μbar (Brown & Ziegler 1979), and during the epoch of perihelion passage, Sedna may have a temporary N<sub>2</sub> atmosphere whose properties depend upon the rotation period, obliquity, and other factors. Triton tholin is a necessary component of the models to reproduce the red spectral slope 0.4–1.0 μm (Cruikshank & Dalle Ore 2003), while amorphous carbon was used to lower the average spectral albedo. The presence of the methanol ice is necessary to better fit the shape of the spectra between 2.2 and 2.4 μm, although we do not see specific absorption bands attributable to CH<sub>3</sub>OH. The large difference in grain size of the constituents makes it difficult to compare the relative abundances of different components. However, it is important to note that the total abundance of different ices is >50%, which is significantly larger than for other TNOs.

## 5. Discussion

The model solution is not unique and depends on many parameters, in particular on the unknown albedo. The possible detection of N<sub>2</sub> and CH<sub>4</sub> would imply a similarity with Triton helping to better understand the origin of Sedna and supporting the capture hypothesis for Triton (McKinnon et al. 1995).

Many hypotheses have been proposed for the genesis of Sedna (Kenyon & Bromley 2004; Morbidelli & Levison 2004; Brown et al. 2004; Stern 2005; Perov 2005) including an extra solar origin. The information presented here on the composition of Sedna will improve our knowledge of the early history of the formation of the solar system. The apparent similarity to Triton could imply a zone of common origin, in agreement with the preferred hypothesis of Morbidelli & Levison (2004) that encounters with other stars perturbed the orbits of some of the solar system's trans-Neptunian planetesimals. In this hypothesis, Sedna was injected into its present orbit by a star passing near our solar system during the earliest stages of formation and before the Kuiper Belt and Oort Cloud originated.

The detection of N<sub>2</sub> (if confirmed) on this distant and large primitive object suggests that N<sub>2</sub> was the dominant form of nitrogen in cold regions of the solar nebula (Owen et al. 2001) and that Sedna is a representative of the icy planetesimals that helped to form the outer planets.

As a consequence of its great current heliocentric distance, Sedna has been minimally processed by solar heating and collisions compared to typical TNOs, but its surface has been heavily processed by galactic cosmic rays causing the formation of red complex organic solids (Strazzulla 1998) which may mask the possible detections of other hydrocarbons. More observations at higher S/N are needed to confirm these results and in particular the geographical compositional variegation on its surface as Sedna rotates. Sedna will become closer and brighter over the next 70 years before it begins to recede in its 10 500-year orbit of the Sun.

*Acknowledgements.* We thank A. Doressoundiram and M. Fulchignoni for helpful discussions and E. Quirico for providing us with some optical constants of ices.

## References

- Barucci, M. A., Belskaya, I. N., Fulchignoni, M., & Birlan, M. 2005, *AJ*, 130, in press
- Barucci, M. A., Boenhardt, H., Dotto, E., et al. 2002, *A&A*, 392, 335
- Barucci, M. A., Doressoundiram, A., & Cruikshank, D. P. 2004, in *Comets II*, ed. M. Festou et al. (University of Arizona Press), 647
- Becker, G. D., Sargent, W. L. W., & Rauch, M. 2004, *ApJ*, 613, 61
- Brown, G. N., & Ziegler, W. T. 1979, in *Advances in Cryogenic Engineering*, ed. K. Timmerhaus, & H. A. Snyder (New York: Plenum Press), 25, 662
- Brown, M. E., Trujillo, C., & Rabinowitz, D. 2004, *ApJ*, 617, 645
- Cruikshank, D. P., Roush, T. L., Owen, T. C., et al. 1993, *Science*, 261, 742
- Cruikshank, D. P., Schmitt, B., Roush, T. L., et al. 2000, *Icarus*, 147, 309
- Cruikshank, D., & Dalle Ore, C. M. 2003, *Earth, Moon and Planets*, 92, 315
- Fornasier, S., Dotto, E., Barucci, M. A., & Barbieri, C. 2004, *A&A*, 422, L43
- Gaudi, B. S., Stanek, K. Z., Hartman, J. D., Holman, M. J., & McLeod, B. A. 2005, *ApJ*, in press
- Gladman, B., Holman, M., Grav, T., et al. 2002, *Icarus*, 157, 269
- Jewitt, D. C., & Luu, J. 2004, *Nature*, 432, 731
- Kenyon, S. J., & Bromley, B. C. 2004, *Nature*, 432, 598
- McKinnon, W. B., Lunine, J. I., & Banfield, D. 1995, in *Neptune and Triton*, ed. Cruikshank (Univ. of Arizona Press), 807
- Morbidelli, A., & Levison, H. F. 2004, *AJ*, 128, 2564
- Owen, T. C., Roush, T. L., Cruikshank, D. P., et al. 1993, *Science*, 261, 745
- Owen, T. C., Mahaffy, P. R., Niemann, H. B., Atreya, S., & Wong, M. 2001, 553, L77
- Perov, N. I. 2005, *Lunar & Plan. Science*, XXXVI, 1049
- Poulet, F., Cuzzi, J. N., Cruikshank, D. P., Roush, T., & Dalle Ore, C. M. 2002, *Icarus*, 160, 313
- Quirico, E., Douté, S., Schmitt, B., et al. 1999, *Icarus*, 139, 159
- Shkuratov, Y., Starukhina, L., Hoffmann, H., & Arnold, G. 1999, *Icarus*, 137, 235
- Stern, S. A. 2005, *AJ*, 129, 526
- Strazzulla, G. 1998, in *Solar System Ices*, ed. B. Schmitt et al. (Netherlands: Kluwer), 281